

## Rock avalanche runout prediction using stochastic analysis of a regional dataset

**Abstract** Rock avalanches involve extremely rapid, flow-like movement of fragmented rock with extreme destructive potential. With increasing development pressures in mountainous regions, there is a need for simple, stochastic estimates of runout distances to aid in hazard assessments and prioritize sites for more detailed investigation. To support the development of an empirical predictive tool, a systematic method was used to describe 49 rock avalanches in the Canadian Cordillera, which had been documented in the literature but not previously compiled into a regional inventory. These cases were described using measured or estimated numerical values for volume, fall height, runout length, total impacted area and the ratio of total impacted area over runout length (referred to as mean path width), and qualitative descriptions of the topographic confinement, substrate material and source geology. Linear regressions were fit to the data, with qualitative attributes treated as indicator variables. A strong relationship was found for runout distance predicted from volume, fall height and lateral confinement. A second relationship was found for mean path width over runout length predicted from volume. These relationships were converted to survival functions to estimate the runout exceedance probability and the mean path width exceedance probability. These survival functions were implemented in a computer tool, called the Probabilistic Runout Estimator—Rock Avalanche (PRE-RA), which can be used to estimate spatial impact probability ranges for rock avalanche runout. An application of this tool was demonstrated using two recent Canadian rock avalanches, which were not used in the dataset to estimate the statistical relationships.

**Keywords** Rock avalanche · Runout · Regression · Stochastic prediction

### Introduction

Rock avalanches are characterized by “extremely rapid ( $> 5$  m/s), massive, flow-like motion of fragmented rock from a large rock slide or rock fall” (Hung et al. 2014). Increasing residential and industrial development in mountainous areas means that more people and infrastructure are exposed to potential rock avalanche hazards, motivating further study to better estimate the mobility of these events. Mitigation of these events is generally not technically or economically feasible, thus risk-based management approaches are typically employed, considering hazard and consequence. To assess the hazard posed by a rock avalanche, the probabilities of several aspects of a potential event must be estimated, including (1) the probability the entire source volume will fail in a single event; (2) the probability the rock mass will fragment and move in a flow-like manner; and (3) the probability the fragmented mass will travel a certain distance, commonly referred to as a runout analysis. This paper focuses on developing empirical methods for performing probabilistic runout analyses.

With a few exceptions (e.g. Mergili et al. 2015), runout analyses, using either empirical or numerical methods, are commonly performed using deterministic analyses. Previously developed empirical relationships for rock avalanche runout based on linear regression have a high degree of variability about the fitted regression lines. Attempts have been made to reduce the variability in the relationships by dividing datasets into categories based on qualitative descriptions of the events and fitting separate regressions to each category (e.g. Nicoletti and Sorriso-Valvo 1991; Corominas 1996; Strom et al. 2019). Probabilistic prediction methods that account for the inherent variability are desirable, particularly in the context of quantitative landslide risk assessment (McDougall 2017). The method described in this paper uses the variability in the observed runout of rock avalanches as a means of characterizing the uncertainty around potential events. The method incorporates qualitative attributes, such as confinement, to improve prediction accuracy.

In many practical situations, screening-level tools are in demand to provide quantitative estimates of rock avalanche travel distance using data that does not require detailed site investigation and characterization. In practice, this situation generally arises when there is a need to prioritize assessment of many hazard sites or determine if more detailed study is warranted. Such tools may also be used to cross-check the results of a detailed study. The objective of this work is to develop a simple probabilistic estimation tool for rock avalanche runout that makes use of qualitative descriptions of the events to refine the mobility estimates. To support this work, a high-quality database of event descriptions, with a focus on attributes that can be reliably described for predictive analysis, has been compiled. Regression models were fitted using the compiled data, which were then used to develop statistical relationships to quantify the variability in the predictions for key runout parameters. The statistical relationships were incorporated into a screening-level predictive tool, called the Probabilistic Runout Estimator—Rock Avalanche (PRE-RA). This tool was developed with geohazard practitioners in mind, who often need to do quick, initial assessments with limited site information.

### Existing tools for practitioners

There are many empirical and numerical runout estimation tools available for practitioners. The focus of this section is primarily on empirical mobility relationships, as those are most commonly used for initial, screening-level assessments.

Empirical measures of rock avalanche mobility have been in use since the pioneering work completed by Albert Heim in the late 1800s and early 1900s. Heim (1932) introduced the concept of *fahrböschung*, or angle of reach, which is the arctangent of the ratio of the fall height,  $H$ , defined as the elevation change from the rock avalanche crest to the furthest runout location, over the travel distance,  $L$ , defined as the planimetric distance following the flow path between those two points (Fig. 1). The physical basis of the

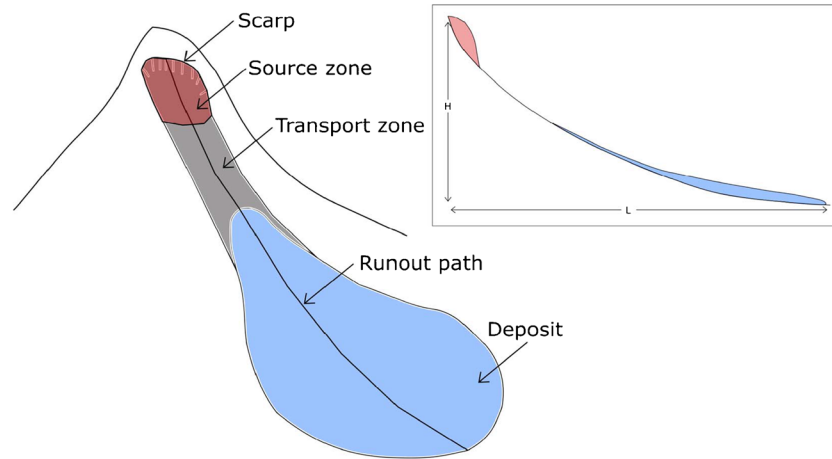


**Fig. 1** Schematic of fall height,  $H$ , and the travel distance,  $L$  (after Heim 1932) and definition sketch showing a schematic of the scarp, source zone (in red), transport zone (in grey) and deposit area (in blue). Total impacted area is the sum of the source zone, transport zone and deposit zone

angle of reach is related to the dynamic sliding friction angle derived from a one-dimensional sliding block analysis, considering conservation of energy (Heim 1932). Heim (1932) found that the angle of reach was inversely proportional to the total volume,  $V$ , of the failed mass for the cases he analyzed.

Many other authors have compiled databases of rock avalanche case histories and presented results in terms of angle of reach (e.g. Scheidegger 1973; Li 1983; Corominas 1996; Hermanns et al. 2012; Zhan et al. 2017). All authors mentioned have found the same inversely proportional trend as Heim (1932), although the slope and intercept of the regressions have varied. Several other parameters, such as deposit area (Li 1983), path topography (Nicoletti and Sorriso-Valvo 1991; Corominas 1996; Strom et al. 2019) and average channel slope (Zhan et al. 2017), have been reported by different authors and incorporated into empirical runout relationships. The impacted area is also an important consideration for assessing the hazard posed by rock avalanche events. Several authors have examined the area covered by the deposit as a function of the volume of the event, either purely empirically (Li 1983; Strom et al. 2019), or constraining the empirical relationships using geometric scaling laws (Hung and Evans 1993; Griswold and Iverson 2008).

The previous empirical studies mentioned above have focused on generating log-linear regression lines or power laws that linearize in log-log space. Examination of the data shows that there is a high degree of variability around the fitted regression lines, especially when consideration is given to the fact that the data is linearized using a logarithmic transformation of both the response and predictor variables. Comparison of the datasets and resulting relationships is complicated by the fact that there is no standard system for describing rock avalanche runout and deposit characteristics.

Empirical relationships to estimate runout have been implemented in a GIS environment to provide a preliminary characterization of potential debris flow and rock avalanche runout scenarios (Griswold and Iverson 2008; Horton et al. 2013; Mergili et al. 2015). Empirical relationships for deposit area and cross-sectional flow area as a function of event volume were used by Griswold and Iverson (2008) in the development of LAHARZ. This

concept was adapted by Simoni et al. (2011) to estimate the potential variability in debris flow events using uncertainty factors on the regression coefficients used to estimate deposit and cross-sectional areas. The approach taken by Horton et al. (2013) was to consider susceptibility to impact based on flow routing and simple, friction-based propagation rules to determine runout length, without explicitly considering an event volume. Mergili et al. (2015) used a constrained random walk methodology for flow routing, with a variety of empirical relationships, such as angle of reach, to estimate when stopping occurs. In the latter two examples, the stopping criteria to determine the propagation of each path are treated deterministically. However, multiple flow paths are combined, using the variability in the flow routing and potentially different regression coefficients for the stopping criteria for different paths, as a means to estimate the potential variation in the runout length and impacted area after aggregating many runs.

A number of advanced numerical models have been developed for the purpose of predicting the runout of rock avalanches or other flow-like landslides (e.g. Hung and McDougall 2009; Christen et al. 2012; Mergili et al. 2017; Wang et al. 2017; Xu et al. 2019). These models are generally used for detailed assessments of potential rock avalanches, and there is generally insufficient data to build and calibrate one of these models for a screening-level assessment. The specifics of the numerical models and their assumptions will not be discussed in detail here.

There is still a need for improved tools that allow for a rapid assessment of the variability in runout. In this study, we developed linear regressions for travel distance and a simplified representation of the total impacted area. The error distributions of those regressions were used to develop equations that can be used to make a stochastic prediction of mobility, accounting for the variability in travel distance and impacted area directly, with only topographic information required. The analysis uses a user-specified path, which allows the examination of large run-up events that can be challenging to address in flow routing-based analyses.

Two types of analyses can be carried out with the PRE-RA predictive tool: path analysis and point analysis. Both analyses

use a user-input path, topography and the stochastic predictive equations. The path analysis option can be applied when a potentially unstable source zone and volume are identified, and there is a need to estimate probabilities of the impacted length and mean width for a potential travel path originating from the source. The point analysis option can be applied when an element at risk is present at a known location near a potentially unstable source zone, and an estimate of the failure volume corresponding to a certain probability of runout exceedance is required. This scenario generally arises when a practitioner is tasked with determining if there is a credible volume that could cause an impact to an element at risk, which is a scenario that has not been directly addressed in previous empirical runout estimation tools.

## Methodology

### Data compilation

To support the development of the regressions and predictive equations, a systematic method was developed to describe rock avalanches and create a regional inventory of rock avalanches occurring in the Canadian Cordillera. The Canadian Cordillera refers to the mountainous region extending from the foothills of the Great Plains in the east to the Pacific Ocean on the west, with the border with the continental USA forming the southern boundary and the border with Alaska forming the northwestern boundary, as shown in Fig. 2. The mountain belts within this region formed as a result of plate convergence along the western edge of the North American Plate, leading to the accretion of offshore arcs and back arc basins, tectonic uplift and extensive volcanic activity through the Jurassic and Cretaceous periods (Monger and Price 2002). Through the Pleistocene, there has been extensive reworking of the landscape during multiple glacial advances and retreats (Clague 2000). Deglaciation within this area happened within the past 10,000 to 14,000 years (Clague 2017), providing a maximum age for landslides with observable deposits. Several notable rock avalanches have occurred in this region within recorded history, including the 1903 Frank Slide (Cruden and Krahn 1973), 1965 Hope Slide (Matthews and McTaggart 1978) and 2010 Mount Meager landslide (Guthrie et al. 2012). A total of 49 cases that have been documented in the literature, but not previously compiled into a regional inventory, were selected. The locations of the case studies are shown in Fig. 2.

The dataset focusses on events that have relatively well-preserved deposits that exhibit characteristic features of flow-like motion. Quantitative measurements of the deposit areas and runout profiles were digitized using Global Mapper software (Blue Marble Geographics 2018). The ASTER version 2 Global Digital Elevation Model (GDEM) was used for all cases for consistency. The measured values that were used for the statistical analysis were checked against the values reported in the references, where available, for validation purposes. Qualitative descriptions of the path topography were made using terminology consistent with Strom et al. (2019). The descriptions of path substrate material were made using terminology consistent with Aaron and McDougall (2019), noting that cases where the rock avalanches are known to involve a significant amount of snow and ice have been excluded from this dataset. The substrate conditions were assessed using descriptions of the substrate material where given in the references or by visual interpretation of the

runout path. Events with a significant splash zone or large volumes of observed entrainment were interpreted to involve saturated substrate (Hungr and Evans 2004). Since many events overran multiple substrate materials, the criterion for determining the representative substrate material was the substrate within the impacted area that would be considered excess mobility (angle of reach  $> 32^\circ$ ) (Hsü 1975). The description of source geology was made using the criteria proposed by Whittall et al. (2017) for distinguishing between strong/fresh and weak/weathered rock masses. The information obtained for this dataset is summarized in Table 1.

The event volumes reported in the references were not re-examined as part of this study. The volumes have been estimated using a variety of methods, and often without the expected error in the estimates reported. The uncertainty associated with the volume estimates and potential implications for the results of this study are examined in the “Discussion” section.

As summarized in the “Existing Tools for Practitioners section”, most studies on rock avalanche area focus on the deposition zone. In this study, we have gathered information on the total impacted area. One reason for this approach is that the boundary between the transport zone and deposition zone is often unclear as a result of vegetation growth, subsequent rock fall activity and erosion, especially for the prehistoric events (temporal uncertainty classes 2 and 3). The other reason is that, from a hazard assessment standpoint, any area impacted by a rock avalanche is of concern, not just the deposit area.

Rock avalanches can mobilize saturated sediments encountered along their travel path, resulting in more fluid and mobile deposits downslope and along the flanks of a coarse, boulder deposit (e.g. Heim 1932; Cruden and Hungr 1986; Hungr and Evans 2004; Orwin et al. 2004). The dataset described in this paper has a mix of older deposits, where evidence of saturated sediment mobilization is not well preserved, and modern deposits with post-event aerial imagery and/or detailed field investigations. For consistency, the digitized deposit areas and runout paths include only the coarse, rocky deposits, as shown in Fig. 3, which are expected to be identifiable in the topography in the future. Inconsistencies in the method to determine the travel distance are the most common source of differences between the referenced literature and the values that are used for the analyses detailed in this paper. For example, the runout length of the Zymoetz River Rock Avalanche shown in Fig. 3 was described by Boulton et al. (2006) as 4200 m, which includes the area shown as mobilized sediment, whereas for this analysis, the runout distance specific to the coarse deposit zone was measured as 1220 m. Ongoing fluvial processes are affecting the channel, and the impacted area along the channel is much less apparent now, even less than 20 years after the event. If an event were to bulldoze coarse colluvium at the foot of the slope that would likely be identifiable in the imagery or topography long term, similar with coarse material that may be rafted on top of a more fluid bed.

The delineation of the deposits for this study was done in an attempt to map the features in historic events that we interpret will be identifiable in the future, so that we can directly compare those runout distances and total impacted areas to the prehistoric deposits. The validity of this approach was supported by the lack of statistically significant differences in fitted models when considering the prehistoric events and historic events separately, as detailed in the “Results” section.



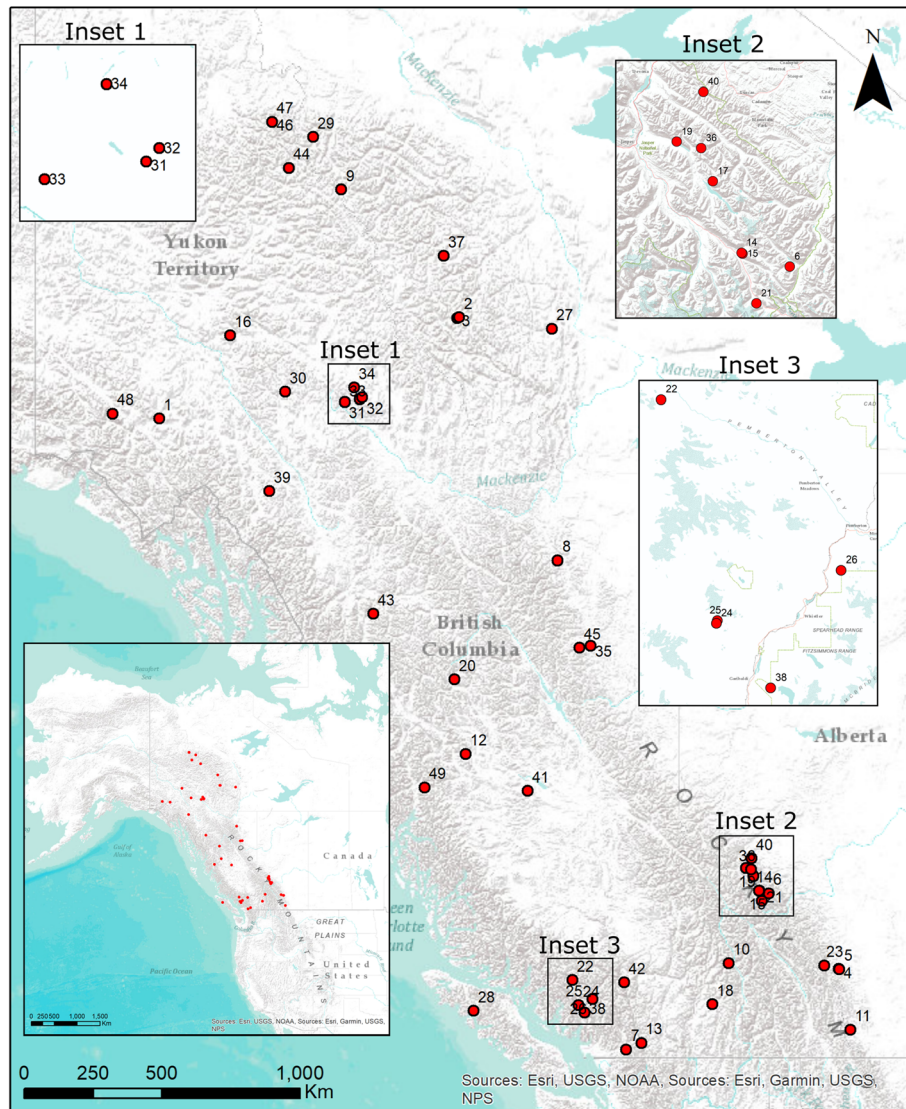


**Fig. 2** Location of study area and rock avalanches included in this dataset. The numbers correspond to the numbers given in the complete dataset (included as Supplemental Material)

### Regression analysis

Several analyses were explored to find statistical models of the variation in runout length and total impacted area predicted from the attributes in the dataset of Canadian Cordillera rock avalanches. A simple approach of applying a linear regression to the H/L ratio (tangent of the angle of reach) versus volume was conducted using logarithmically transformed data for the predictor and response variables. A multiple linear regression was also fit by treating the volume and fall height as separate predictors of runout length, using logarithmic transformations of all three variables (similar to the graphical analysis presented in Li 1983). An analysis of the residuals of the linear regressions was completed to examine potential clustering or stratification of the data. Box plots of residuals for each of the descriptive factors outlined in Table 1 were generated and used to evaluate whether a difference in the behaviour of the events could be observed on the basis of these factors.

Following the exploratory analysis, the descriptive factors that showed the strongest stratification in the box plots were included in the linear regressions as indicator variables. An indicator variable is a binary variable that is 1 if the condition is true and 0 if it is false (Young 2017). For example, if a regression was generated using saturated substrate as an indicator variable, the regression would use all of the data in the dataset; however, the saturated cases (where the indicator variable has a value of 1) would have an offset applied to the regression to account for the different mobility of these cases. An advantage of this approach versus generating separate regressions for each factor is that it does not require subdividing the dataset, and there are estimation efficiency gains because fewer parameters generally need to be fitted using the entire dataset. The regression model for runout distance we considered is written as:

$$\log L = \beta_0 + \beta_1 \log V + \beta_2 \log H + \beta_3 C + \varepsilon \quad (1)$$



**Table 1** Attributes and sources of information used to describe events included in the dataset

	Attribute	Units/descriptor	Source/comments
Quantitative	Volume	M m <sup>3</sup>	Published references
	Fall height	m	ASTER GDEM v2
	Travel distance	m	Digitized path
	Total impacted Area	m <sup>2</sup>	Digitized deposit
Qualitative	Path topography	Unconfined	Visual interpretation of deposit shape and topographic features in the impacted area
		Laterally confined	
		Frontally confined	
	Path substrate	Saturated	Published references, if available, or visual interpretation of landforms from aerial/satellite imagery
		Unsaturated	
		Bedrock	
	Source geology	Weak/weathered	Published references, if available, or estimated from publicly available geological maps
		Strong/fresh	
	Temporal uncertainty	0—known	Date of event from eyewitness reports, daily satellite imagery and/or seismic signal
		1—well constrained	Year of event from eyewitness accounts or aerial photographs
		2—moderately constrained	Approximate age from radio carbon or cosmogenic nuclide dating
		3—approximately constrained	General geologic/geomorphic evidence available (e.g. post-glacial)

where  $L$ ,  $V$  and  $H$  are as defined in the “Existing tools for practitioners” section;  $\beta_0$ ,  $\beta_1$ ,  $\beta_2$  and  $\beta_3$  are the regression coefficients;  $C$  is an indicator variable (0 or 1) and  $\varepsilon$  is the error term, assumed to be normally distributed with zero mean,  $\varepsilon \sim N(0, \sigma^2)$ .

The impact area for the coarse fractured rock debris was also considered, and a linear regression of the logarithm of volume versus the logarithm of the total impacted area was generated. A challenge with using the impacted area is predicting the shape of the deposit. A simple metric of the spreading of an event can be estimated using the mean path width, found by dividing the total impacted area by the runout length. The logarithm of mean path width ( $W$ ) was compared with the logarithm of event volume. The variability in the data was quantified by fitting a normal distribution to the regression residuals. The regression model for the mean path width is written as:

$$\log W = \beta_0 + \beta_1 \log V + \varepsilon \tag{2}$$

where all terms are as defined previously.

### Predictive analysis

The two linear regression models given in Eqs. (1) and (2) were used to develop stochastic predictive equations. The key assumption is that the models in Eqs. (1) and (2) capture the range of potential outcomes of future events. Relying on the assumption of the normally distributed error term,  $\varepsilon$ , we can rearrange the linear regression equation into the form of a survival function (Young 2017). The survival function for the travel distance derived from Eq. (1) is written as:

$$P(L \geq l | H = h, V = v, C = c) = 1 - \Phi \left( \frac{\log l - \beta_0 - \beta_1 \log v - \beta_2 \log h - \beta_3 c}{\sigma} \right), l > 0 \tag{3}$$

where  $l$ ,  $h$ ,  $v$  and  $c$  are given values for runout distance, fall height, volume and lateral confinement (true or false), respectively;  $\Phi$  is the cumulative distribution function for a standard normal variable.

Likewise, the survival function derived from Eq. (2) follows the same format and is written as:

$$P(W \geq w | V = v) = 1 - \Phi \left( \frac{\log w - \beta_0 - \beta_1 \log v}{\sigma} \right), w > 0 \tag{4}$$

where  $w$  is a given value for mean path width; all other terms are consistent with Eqs. (2) and (3).

The values of  $P(L \geq l | H = h, V = v, C = c)$  and  $P(W \geq w | V = v)$  are referred to as runout exceedance probability and mean width exceedance probability, respectively, throughout this paper.

### Implementation

The survival functions given in Eqs. (3) and (4) have been implemented in the PRE-RA predictive tool. In the path analysis option, the PRE-RA tool provides estimates of the runout exceedance probability and the mean width exceedance probability at multiple points along a user-defined path. In the point analysis option, the tool provides an estimate of the minimum failure volume required to result in a specified runout exceedance probability at a specified

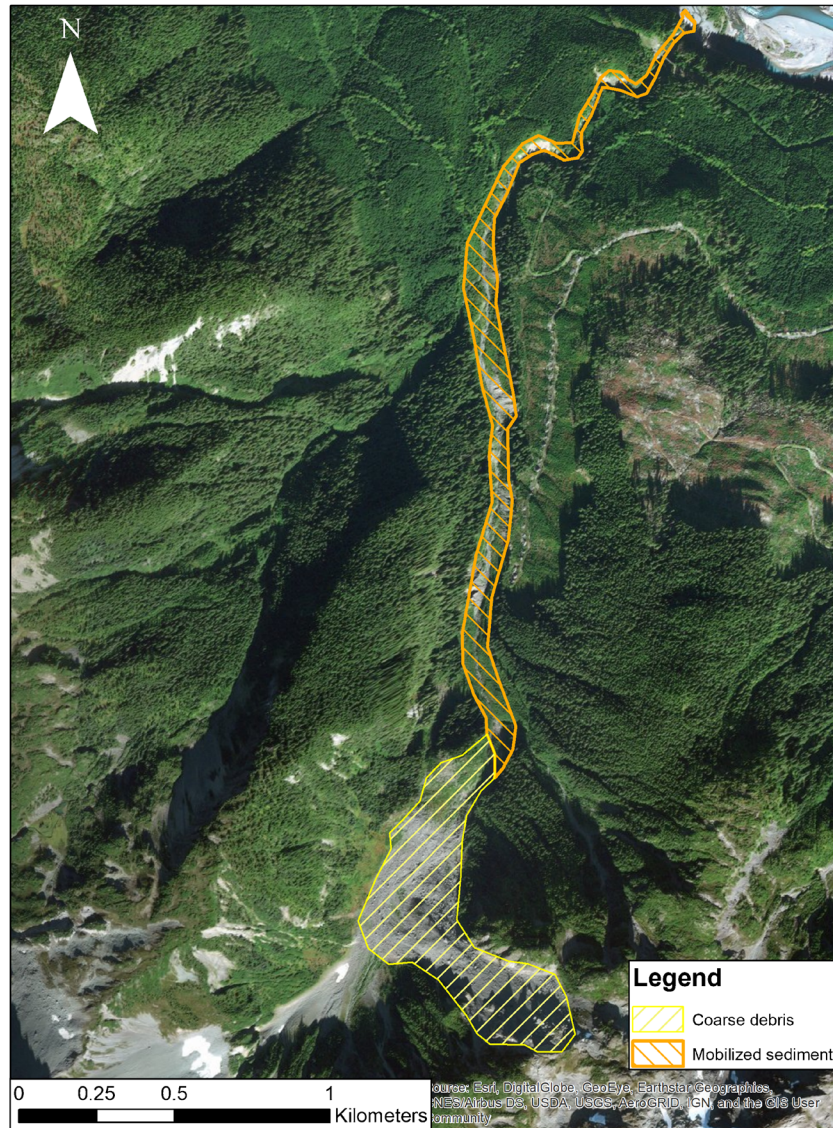


**Fig. 3** Example of separation of coarse rocky deposits from the channelized sediments that were highly mobile for the 2002 Zymoetz River Rock Avalanche

point (typically corresponding to the location of a key element at risk). The graphical representation and statistical analyses for both the path analysis and point analysis types have been implemented in R (R Core Team 2018).

The workflow for the PRE-RA program is summarized in Fig. 4. Both analysis types start in the same way, with separate linear regressions fit to the data for travel distance and mean path width based on the data from the 49 Canadian Cordillera rock avalanche cases. The estimates of regression coefficients and error distribution standard deviations for the data are then obtained. A digital elevation model (DEM) with northing and easting values in metres is provided by the user. The DEM is read into the program, and a hillshade representation is generated, onto which the user digitizes a runout path. The program extracts the elevation data from the DEM at each digitized point and calculates the 2D profile to obtain the change in elevation from the top of the path to each digitized point ( $h$ ), and the path distance from the source ( $l$ ) in metres.

A potential landslide volume, in  $M \text{ m}^3$ , is entered by the user for the path analysis option. The runout exceedance probability at each digitized point along the travel path is calculated using Eq. (3). The runout exceedance probability is presented as a range instead of exact values as a way of demonstrating the uncertainty inherent in the analysis. The values along the profile corresponding to the set end points of the probability ranges are found using linear interpolation. Once the points are found on the 2D profile, the equivalent points along the 3D path are found and plotted on the topography. The mean deposit width is estimated from the event volume using Eq. (4) and applied as an offset on either side of the digitized runout path.

The point analysis iteratively solves Eq. (3) by adjusting  $v$  so that it produces the calculated  $P(L > l_f | H = h_f, V = v, C = c)$  for the last point on the runout profile ( $l_f, h_f$ ). The calculated minimum failure volume is output along with a plot of the runout path.

The version of the predictive tool presented here only uses the Canadian Cordillera rock avalanche dataset with the multiple

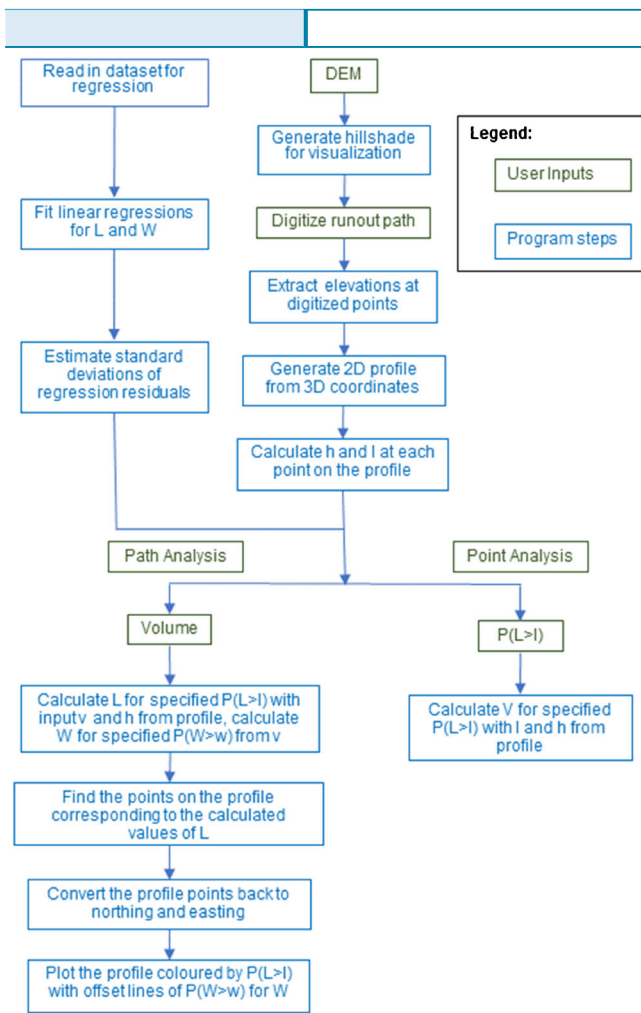


Fig. 4 Flowchart for the PRE-RA predictive tool

linear regression for the logarithm of runout length, and a simple linear regression for the logarithm of mean path width. Mitchell et al. (2018) presented an earlier version of this tool, which used several datasets published by other authors and H/L as the basis for runout probability estimation.

## Results

### Dataset

The events included in the Canadian Cordillera dataset range from 0.1 to 500 M m<sup>3</sup>. The fall heights range from 220 to 1720 m, and the runout distances range from 950 to 8950 m, with H/L ranging from 0.12 to 0.6 (angle of reach of 7° to 31°). A summary table of all cases, attributes and references is included as [Supplementary Material](#). The precision of the measured attributes is dependent on many factors, including the age and preservation of the deposit, vegetation cover, topographic data quality and resolution, and imagery quality, and a detailed estimation of the limit of precision or measurement accuracy has not been completed. To recognize the limited precision possible in these measurements, runout distances and fall heights are reported to the nearest 10 m, and volumes are reported to two significant figures.

## Regression analyses

### Travel distance

The simple linear regression of log-H/L versus log-volume is shown in Fig. 5. A multiple linear regression with log-volume and log-fall height as predictors of log-runout distance was fit, and an exploratory analysis was carried out by making box plots of the residuals from the multiple linear regression for L using the descriptive factors included in the database (Table 1), provided as [Supplementary Material](#). The results indicate that frontal confinement tends to reduce mobility, while lateral confinement enhances it, and unconfined cases are relatively unbiased compared with the overall regression. Unsaturated substrates tend to have less mobility; however, the sample size is small, reducing our ability to quantify this potential relationship. No clear stratification of the residuals can be observed for the source geology. From this visual analysis, amongst the descriptive factors included in the database, topographic confinement has the strongest effect on the residuals.

Following the finding that confinement was a strong control on mobility for this dataset, new multiple linear regression models were fit using lateral and frontal confinement as indicator variables. A summary of the regression fit statistics for these analyses is provided in Table 2. The adjusted R<sup>2</sup> value is higher and the standard error is lower on all coefficients for the regression using lateral confinement as the indicator variable, indicating this is the stronger statistical relationship compared with frontal confinement. The regression surfaces for lateral confinement being true and false are shown in Fig. 6.

The assumption that the prehistoric events (temporal uncertainty classes 2 and 3, described in Table 1) were comparable with the rest of the dataset where only the coarse debris was mapped was tested by fitting separate regression models to subsets of the data separated into temporal uncertainty classes 0 and 1 (historical events with better preserved deposits and often evidence of impacts beyond the coarse, rocky debris preserved) and temporal uncertainty classes 2 and 3 (included as [Supplemental Material](#)). For this analysis, confinement was not used as a predictor. The results showed no significant difference between the regression models fit to the two subsets at a 95% confidence level, supporting the assumption that the various ages of deposits can be grouped together for this analysis using the deposit mapping methodology described in this paper.

### Mean path width

A simple linear regression of log-total impacted area versus log-volume was fit, which indicated strong associations between log-area and log-volume, as well as a multiple linear regression using log-area predicted from log-volume and log-fall height (included as [Supplemental Material](#)). To simplify the predictive process, regressions using a simplified measure of the area, represented by the mean path width, were fit. The simple linear regression of mean path width versus event volume is shown in Fig. 7. The associated regression fit summary is shown in Table 3. There is a strong correlation between the volume and the mean deposit width. Multiple linear regression models with width predicted from runout length and volume or from fall height and volume were fitted, but the association was less strong than the simple linear regression, as summarized in Table 3. An exploratory



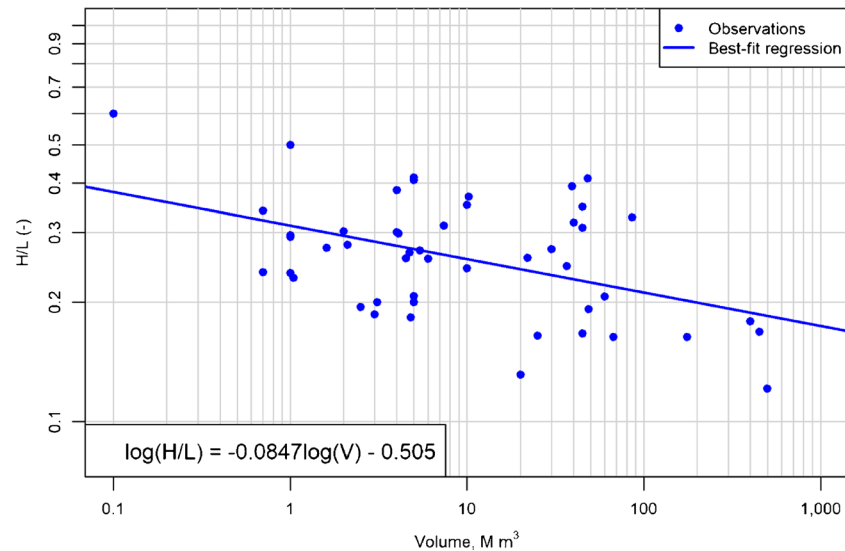


**Fig. 5** Linear regression of H/L predicted from event volume (V) for 49 rock avalanches in the Canadian Cordillera

analysis was carried out by making box plots of the residuals from the simple linear regression for W (Supplemental Material) using the descriptive factors included in the database (Table 1). Clear stratification of the residuals was not observed in this dataset. Weak stratification was noted for path topography; however, the statistical association was not strong when confinement was used as an indicator variable.

#### Error analysis

The predictive analysis uses the assumption that errors are normally distributed with zero mean. To assess this assumption, Fig. 8 shows histograms as well as Q-Q plots for the residuals from the regressions used in the predictive analysis and, for comparison, from the regression of H/L versus volume. The error distributions for both the multiple linear regression for runout length and the simple linear regression for mean path width appear to be closer to a normal distribution than the simple linear regression of H/L versus volume, especially visible in the assessment of the tail behaviour through Q-Q plots.

#### Predictive analysis

The coefficients found for the regression using lateral confinement as an indicator variable (Table 2) and the standard deviation of the residuals, as an estimate of  $\sigma$ , were substituted into Eq. (3) to produce the following survival function to estimate the mean width exceedance probability for the Canadian Cordillera dataset:

$$P(L \geq l | H = h, V = v, C = c) = 1 - \Phi\left(\frac{\log l - 1.412 - 0.139 \log v - 0.640 \log h - 0.169c}{0.105}\right), l > 0 \quad (5)$$

The coefficients found for the regression of mean path width (Table 3) and the standard deviation of its residuals were substituted into Eq. (4) to produce the following survival function to estimate the mean width exceedance probability for the Canadian Cordillera dataset:

$$P(W \geq w | V = v) = 1 - \Phi\left(\frac{\log w - 2.327 - 0.325 \log v}{0.156}\right), w > 0 \quad (6)$$

**Table 2** Summary of regression fit statistics

	Simple linear regression		Multiple linear regression		Multiple linear regression—frontal confinement		Multiple linear regression—lateral confinement	
	Estimate	Standard error	Estimate	Standard error	Estimate	Standard error	Estimate	Standard error
Adjusted $R^2$	0.19		0.71		0.76		0.80	
$\log(V)^a$	-0.0847	0.0239	0.105	0.026	0.136	0.026	0.139	0.023
$\log(H)^a$	NA	NA	0.807	0.109	0.732	0.104	0.640	0.098
C	NA	NA	NA	NA	-0.114	0.037	0.169	0.037
Intercept	-0.505	0.030	1.027	0.297	1.260	0.284	1.412	0.262
$\sigma$	0.132		0.128		0.116		0.105	

<sup>a</sup> See Table 1 for units

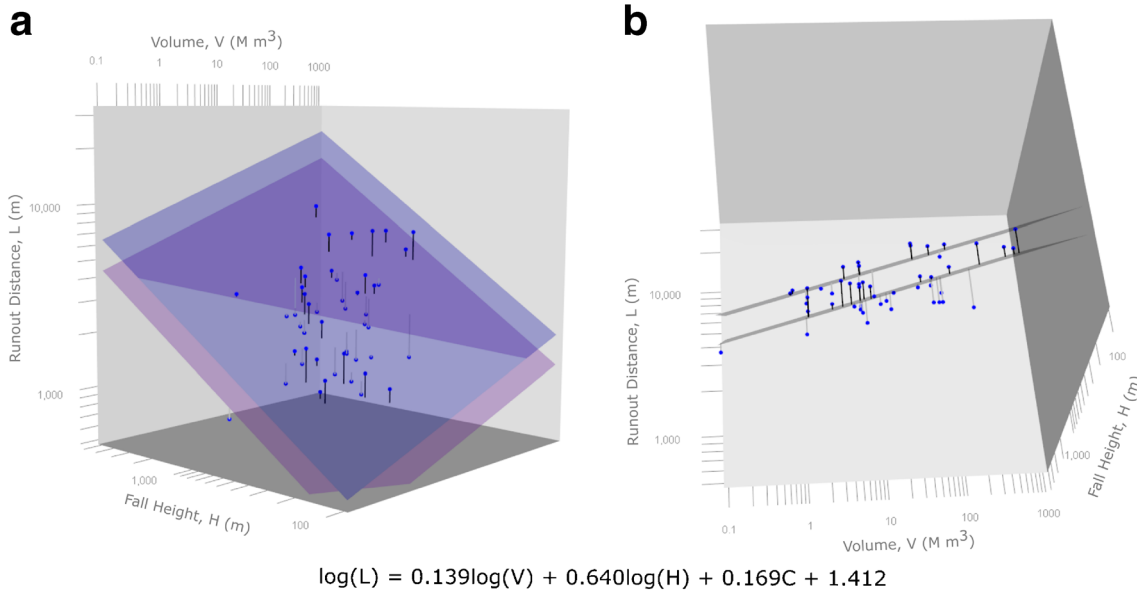


**Fig. 6** Multiple linear regression using lateral confinement as an indicator variable (C), showing **a** runout distance (L) predicted by event volume (V) and fall height (H), and **b** a rotated view to show the magnitude of the residuals (right panel). The upper (blue) surface is the fit surface when lateral confinement is true, and the lower (pink) surface is the fit surface when lateral confinement is false

A sensitivity analysis was completed by evaluating the probability of exceedance for a range of runout distance values at fixed fall heights, volumes and lateral confinement conditions. The values chosen for plotting, shown in Fig. 9, span the range of most fall heights and volumes in the dataset. The zone where the travel angle is greater than 32°, corresponding to Hsü's (1975) definition of excess mobility, is also shown.

### Example analysis

A demonstration of the PRE-RA tool developed in this study is shown using the 2019 Joffre Peak Rock Avalanches in British Columbia (Friele et al. press). One rock avalanche occurred on

May 13, 2019, and a second rock avalanche from an adjacent area on the rock face occurred on May 16, 2019. Both events originated from the northeast face of Joffre Peak, and travelled down a laterally confined path. The runout lengths and areas reported here were estimated using 3-m pixel size satellite imagery collected on May 13, 2019, and May 30, 2019 (Planet Team 2017). Elevation data were obtained from the Canadian Digital Elevation Model (CDEM) Mosaic for the area between 50° 20' 20.6" and 50° 23' 19.7" north latitude and 122° 23' 42.1" and 122° 27' 32.3" west longitude. Volumes of the two events were estimated by comparing photogrammetry models of the pre-event topography in 2017: the post-first event topography collected on May 15, 2019 and the post-

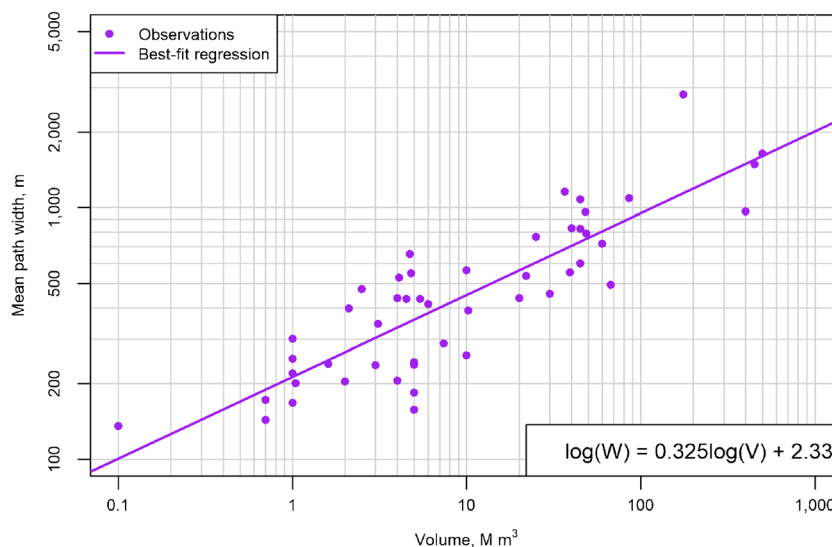


**Fig. 7** Mean runout path width versus rock avalanche volume relationship for the 49 Canadian Cordillera rock avalanches considered in this study

**Table 3** Summary of simple linear regression fit statistics for mean runout path width versus rock avalanche volume relationship

	Simple linear regression		Multiple linear regression		Multiple linear regression	
	Estimate	Standard error	Estimate	Standard error	Estimate	Standard error
Adjusted $R^2$	0.73		0.73		0.73	
Coefficients						
$\log(V)^a$	0.325	0.028	0.335	0.032	0.340	0.037
$\log(H)^a$	NA	NA	-0.099	0.133	NA	NA
$\log(L)^a$	NA	NA	NA	NA	-0.078	0.122
Intercept	2.327	0.035	2.593	0.362	2.576	0.392
$\sigma$	0.156		0.155		0.156	

<sup>a</sup> See Table 1 for units

second event topography collected on May 18, 2019. Features of this rock avalanche are summarized in Table 4. The rock avalanche deposits, paths and profiles are shown along with key geographic features in Fig. 10.

The CDEM elevation grid data were converted to a UTM grid using Global Mapper software. A path analysis was run for event volumes of 2 M m<sup>3</sup> and 3 M m<sup>3</sup> with lateral confinement set as true. A path was digitized from the crest of each event's head scarp, following the actual deposit, then extending down the Cerise Creek drainage to where it joins with Cayoosh Creek. Output of the analyses for the runout exceedance probability at any point along the digitized path, as well as offsets showing the range of path width exceedance probabilities, are shown in Fig. 11. The runout and mean path width values for each analysis are provided in Table 5.

A point analysis, performed to estimate the volume required for a potential future failure to dam Cayoosh Creek, was run along the May 16, 2019 event path (Fig. 12). The algorithm used to perform a point analysis is summarized in the "Implementation" section. An arbitrary target of  $P(L > l_f | H = h_f, V = v, C = c) = 0.25$ , where  $l_f = 5700$  m,  $h_f = 1440$  m and  $c = 1$ , was selected for this analysis. The

minimum failure volume estimated from this analysis, assuming lateral confinement, is 4 M m<sup>3</sup>. Therefore, an event with a volume of 4 M m<sup>3</sup> is estimated to have a probability of 0.25 of travelling as far as Cayoosh Creek. Smaller volume events are estimated to have a probability less than 0.25 of reaching this point given the conditions above.

### Discussion

A marked improvement is noted in the strength of the associations using fall height and volume as separate variables in the model to predict runout distance (Table 2), consistent with the findings of Zhan et al. (2017). Furthermore, the predicted runout distances were found to be highly sensitive to the fall height, as shown in Fig. 9. This generally agrees with the results of Nicoletti and Sorriso-Valvo (1991), who found fall height was a stronger predictor than volume when performing a simple linear regression. The relative magnitudes of the coefficients also generally agree with the results of Zhan et al. (2017). These findings are contrary to the conclusions of Legros (2002), who suggested that long travel distances were primarily related to local slope and volume. Analyses of residuals of the H/L and runout length versus fall height

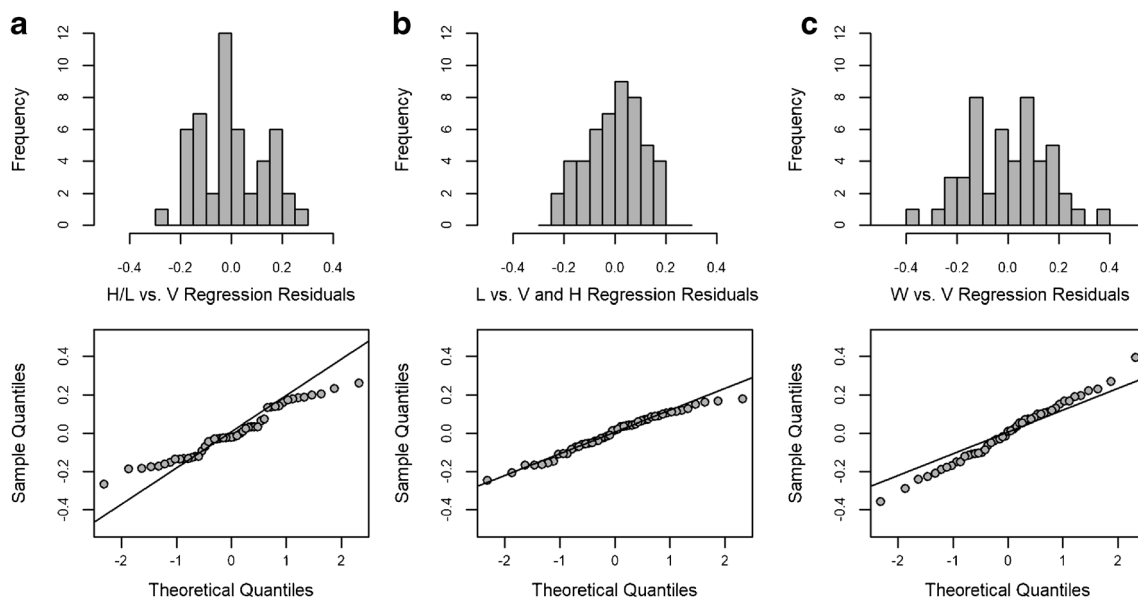


**Fig. 8** Histograms of regression residuals (top row) and normal Q-Q plots (bottom row) for **a** the simple linear regression for H/L, **b** the multiple linear regression for L and **c** the simple linear regression for W



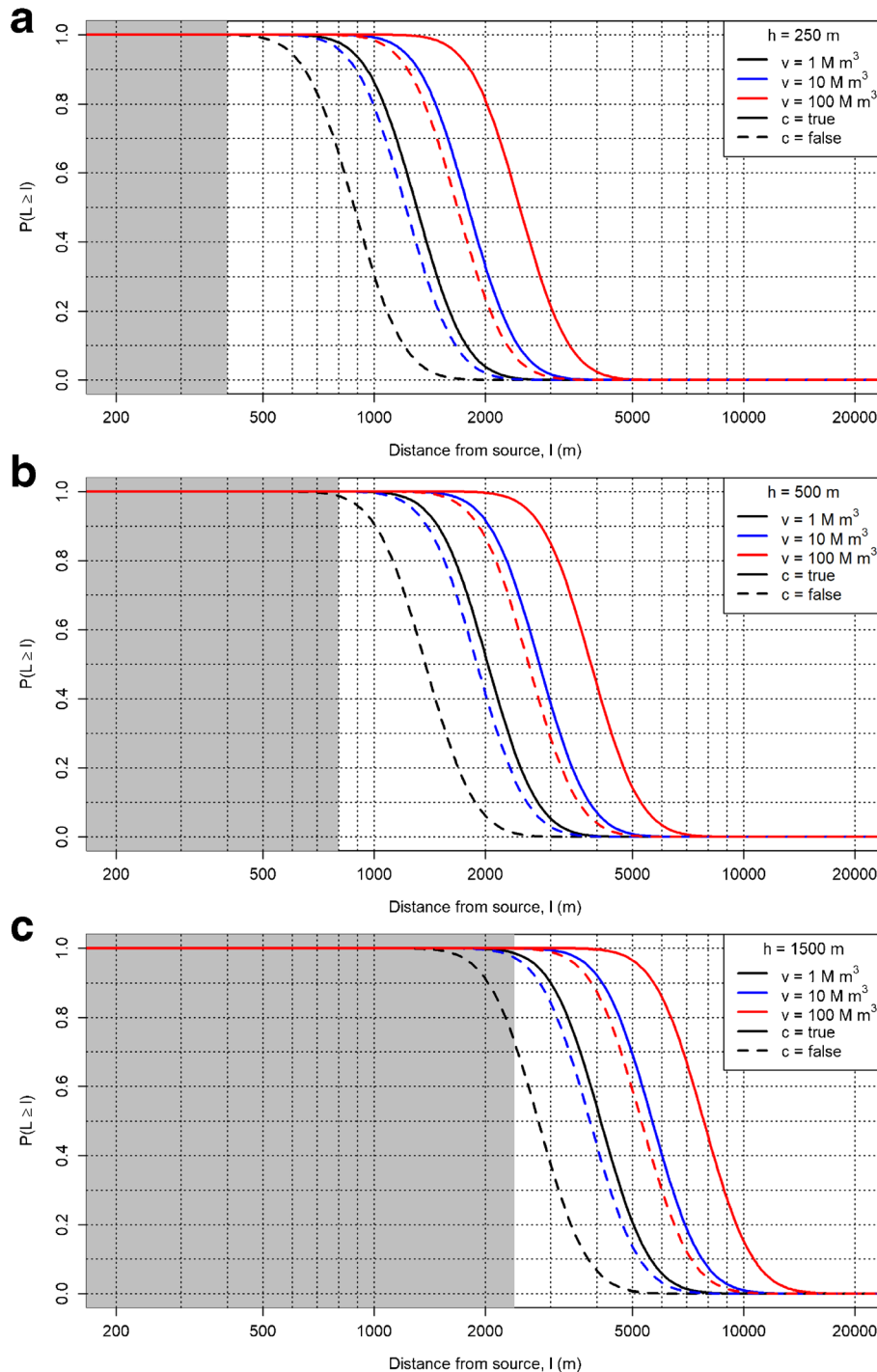


**Fig. 9** Parametric plots showing the relationship between runout exceedance probability with increasing distance from the source area at fixed values of fall height and volume, for the Canadian Cordillera dataset. Solid lines indicate lateral confinement, and dashed lines are unconfined or frontally confined. The grey zone indicates where the angle of reach for the given fall height is less than  $32^\circ$

and volume analyses in this study show path topography has the strongest effect on the residuals, with unconfined paths generally well described by the regression, lateral confinement having enhanced mobility and frontal confinement having limited mobility (Table 2).

There is potential for some of the factors examined in this study to be inter-related. For example, laterally confined cases tend to

run out further, generally following valleys, thus they are more likely to have saturated substrate. Numerical modelling work looking at the effect of path substrate on the mobility of back analyzed events showed a similar trend of saturated substrate tending to enhance mobility relative to unsaturated substrate (Aaron and McDougall 2019). In that study, the effect of substrate was likely stronger on the clustering of results, as the model that

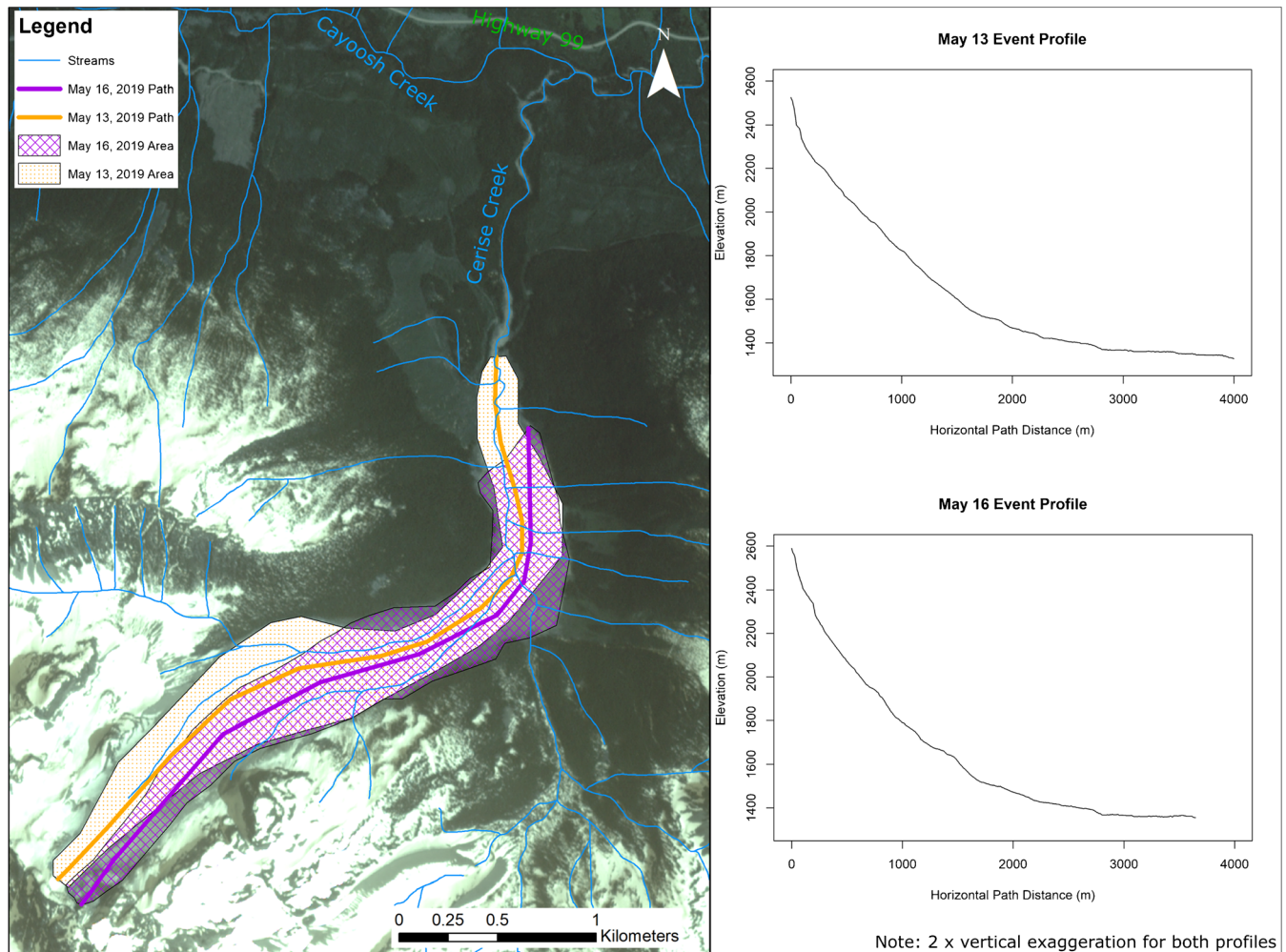
**Table 4** Geometric characteristics of the Joffre Peak rock avalanches

Event	May 13, 2019	May 16, 2019
Volume (M m <sup>3</sup> )	2	3
Runout distance (m)	4000	3650
Fall height (m)	1200	1300
Area (m <sup>2</sup> )	$1.27 \times 10^6$	$1.15 \times 10^6$
Mean path width (m)	320	315

was used explicitly considers the effect of the 3D terrain variation. Analysis of runouts in open-pit settings found good clustering of the results based on the source geology (Whittall et al. 2017), which was not observed in this analysis of natural rock avalanches. The runout path topography and substrate conditions tend to be much less variable in open-pit settings than they are in natural rock avalanche paths, thus the effects of source geology may have a stronger expression. The analysis of the rock avalanche cases presented in this paper suggests that path confinement is a reliable qualitative predictor of mobility, which is consistent with the work

of Nicoletti and Sorriso-Valvo (1991), Corominas (1996) and Strom et al. (2019). With a larger dataset of consistently described events, a hierarchy of factors could be developed to help guide practitioners in decisions on what factors to prioritize for investigation to refine runout estimates, such as source volume, topographic relief, path confinement, path substrate and source material.

The relationship between area and volume found for this dataset shows a positive correlation with a strong linear association. Mean path width has been investigated as a way to predict spreading behaviour for a given event volume without performing a flow routing calculation. A positive relationship exists with good statistical strength (Table 3). The simplicity of this analysis is attractive for making screening-level predictions; however, judgement is required to interpret the results. As the prediction is for a mean value, some areas are expected to spread more or less than the predicted value. This is demonstrated in Fig. 11, where the observed spread was significantly outside of the mean width, especially in areas where the rock avalanche went around bends. Significantly wider spreading than the mean value can also be expected at the distal ends of deposits in frontally confined cases or unconfined cases where the mass is free to spread, for example on an open valley floor.

**Fig. 10** Joffre Peak Rock Avalanche deposit areas and profiles overlain on Planet Inc. imagery from May 30, 2019

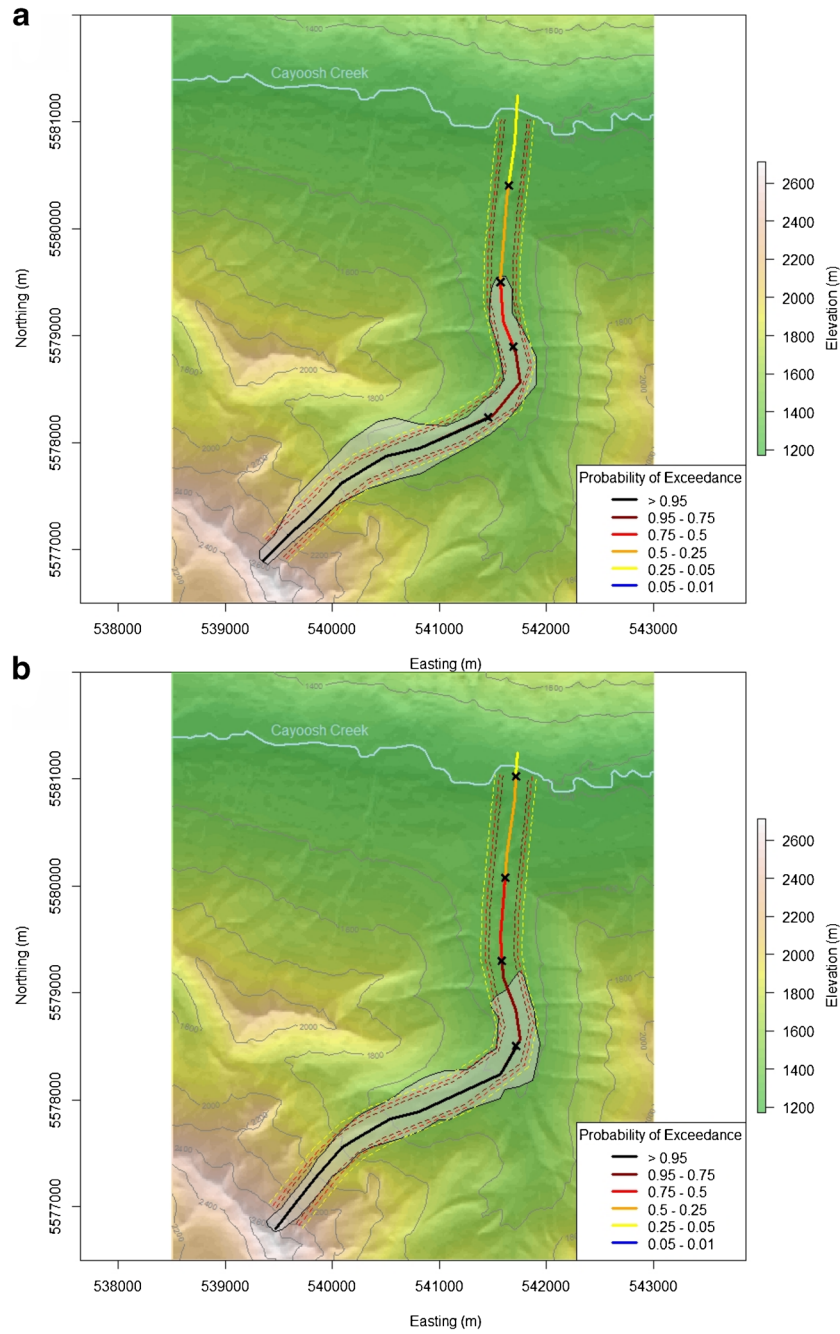


**Fig. 11** Runout exceedance probability along the travel paths of **a** the May 13, 2019 Joffre Peak rock avalanche and **b** the May 16, 2019 Joffre Peak rock avalanche. Both paths were extended past the observed runout, following the Cerise Creek drainage to Cayoosh Creek. The observed deposits of both events are shown by the grey polygons

**Table 5** Observed values and probability ranges for the Joffre Peak rock avalanches

Event	Runout (m) Observed	$P(L > l   H = h, V = v, C = \iota)$				Width (m) Observed	$P(W > w   V = v)$			
		0.95	0.75	0.50	0.25		0.95	0.75	0.50	0.25
May 13, 2019	4000	2550	3330	3950	4860	320	147	208	265	340
May 16, 2019	3650	2920	3750	4530	5480	315	168	238	303	387



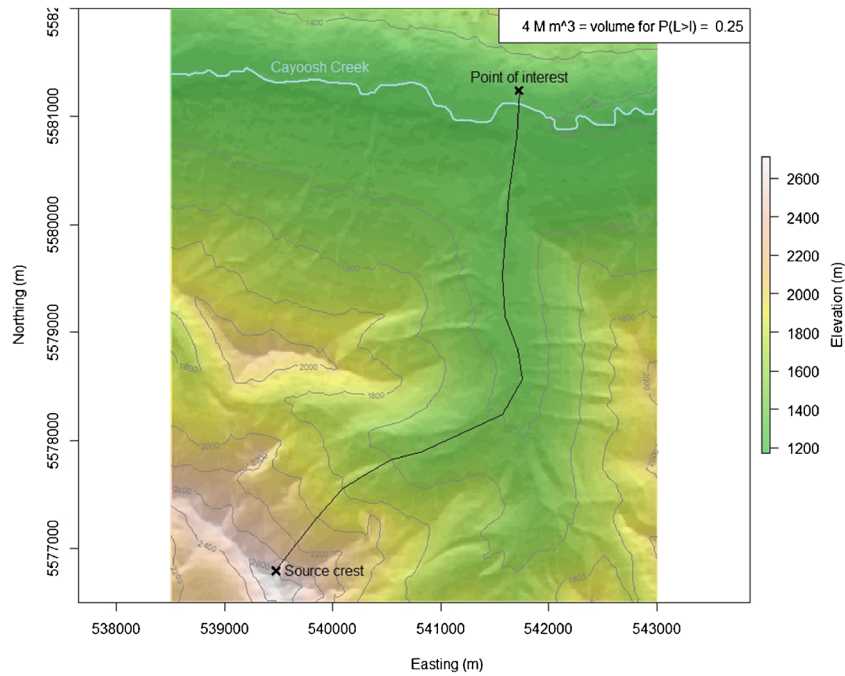


**Fig. 12** Volume output for a specified  $P(L > l_f | H = h_f, V = v, C = c)$  for an event originating from the May 16, 2019 crest location that could have blocked Cayoosh Creek

There is some degree of uncertainty associated with characterizing the rock avalanche volumes, impacted areas, runout lengths and fall heights in the dataset presented. This is especially true for older, eroded and/or overgrown deposits, which are not as clearly defined as more recent events. Since rock avalanches are relatively rare compared with other mass movement processes, eliminating the older events would result in a very limited dataset. An effort was made to limit the effect of the uncertainties by using consistent methods and data sources for topography, and checking values against multiple sources where possible. There is also some subjectivity involved in assigning the descriptive attributes. A common challenge is that more than one descriptor could be applied to many cases. As an example, a failure may start on an open, unconfined slope, enter a confined valley, then spill out onto a broad floodplain and encounter bedrock, unsaturated and saturated sediments along its path. Judgement is needed to assign a representative value for the descriptive factors, and practitioners may need to look at multiple scenarios when performing a forward analysis.

The parameter with the greatest uncertainty is event volume, as very few events have pre- and post-event topographic data available, thus various indirect volume estimation methods were applied by the authors of the referenced case studies. The results of the regression analyses indicate that the predicted runout length has a relatively low sensitivity to volume. For example, using the multiple linear regression presented in Fig. 6 and a hypothetical event with a fall height of 500 m and volume of  $10 \text{ M m}^3$ , without lateral confinement the predicted runout distance would be 1900 m. If the volume was overestimated by a factor of 2, i.e.  $20 \text{ M m}^3$ , the predicted runout distance would be 2090 m or only a 10% difference. The relatively low sensitivity to this variable, and the fact that the predictions focus on ranges of possible outcomes, help mitigate the effect of the uncertainty that generally comes with estimating event volumes, both for back analysis and forward predictive analysis. The

sensitivity analysis (Fig. 9) indicates the strong effect of confinement, where an approximate order of magnitude increase in volume is needed to produce a runout length in a non-laterally confined case equivalent to the runout in a laterally confined case. The point on the curves where the  $P(L \geq l_f | V = v, H = h, C = c)$  values are well below the value of 1 are generally consistent with the minimum  $32^\circ$  angle of reach value proposed by Hsü (1975).

The runout exceedance probabilities are presented as ranges rather than distinct values as a way of recognizing the uncertainty inherent in the data and, as a result, in the analysis. The relatively broad probability ranges output by the predictive tool are appropriate given that it is intended to be used as a screening-level tool. Where this screening-level analysis indicates a sufficiently high probability of impact from a credible rock avalanche event, detailed site investigation and more sophisticated numerical analysis may be completed as a follow-up. The probabilistic outputs presented here can also be used for preliminary risk analysis. The runout probabilities obtained from the analysis are relevant for the bulk of a potential landslide event; however, there may be significant mobilizations of saturated sediments that could form a splash zone or become channelized and have a significantly greater runout (e.g. Fig. 3).

The output of the PRE-RA tool was compared with the observed runout and spreading behaviour of the 2019 Joffre Peak rock avalanches, which followed a laterally confined runout path. The observed runout of the May 13, 2019 event was within the zone where  $P(L > l_f | V = 2 \text{ M m}^3, H = h, C = 1)$  is in the range of 0.50 to 0.25, and the observed runout of the May 16, 2019 event was within the zone where  $P(L > l_f | V = 3 \text{ M m}^3, H = h, C = 1)$  is in the range of 0.95 to 0.75. The observed deposit width for both events was within the zone where  $P(W > w | V = 2 \text{ M m}^3)$  and  $P(W > w | V = 3 \text{ M m}^3)$  are in the range of 0.50 to 0.25. This implies that the mobility and spreading of the first event was within a typical range compared with the other events in the dataset with consideration of

volume, fall height and confinement; however, the travel distance of the second event was relatively low.

The observed behaviour of the two 2019 Joffre Peak events compared with the empirical predictions show some notable differences. Given the volume estimates and fall heights, the second event would be expected to be more mobile based on the relationships presented here, while in reality, the runout distance was slightly less than the first event despite a greater volume and fall height. This could be due to the presence of the first event deposit, which occupied the most efficient path down the slope and provided a rougher surface over which the second event had to travel. Additionally, if a mobility enhancing substrate material was present, it may have been mobilized by the first event and not available to enhance the mobility of the second event.

The results of the point analysis indicate that a failure of over 4 M m<sup>3</sup>, i.e. less than the combined volume of both events, would have a probability of reaching Cayoosh Creek greater than 0.25. If the creek was blocked, it could have important implications for upstream flooding and the potential for a breach of the landslide dam to impact downstream people and infrastructure. The limited mobility of the second event and the plausibility of the combined volume deposit directly impacting Cayoosh Creek highlight the importance of determining if unstable source zones fail as single events or multiple events when performing hazard or risk assessments. Additionally, the presence of snow and ice within the source area of events could have enhanced mobility beyond what would otherwise be expected. Events that clearly ran out over glaciers were excluded from this dataset; however, it is possible that significant amounts of snow and ice were involved in the prehistoric events in the dataset. Associated effects of the rock avalanches, such as the mobilization of sediment and woody debris in the drainage downslope of the deposit (Friele et al. [in review](#)) are also not captured in this analysis, but can have important implications for risks to people or infrastructure.

There may be advantages to converting descriptive variables to continuous numeric variables where possible. One potential path of inquiry could involve morphometric analyses of the runout areas to look for ways to quantify confinement numerically.

This dataset only considers events from the Canadian Cordillera. Consistent simple and systematic descriptions of more events in a wider variety of locations could help to build larger, more statistically robust datasets for future analysis. Larger datasets described in a consistent manner may also help to better determine the effect of some attributes, such as path substrate or source material. Examination of events from other geographic regions could provide further insight on regional factors contributing to rock avalanche runout.

## Conclusions

A simple, screening-level tool to provide geohazard practitioners with stochastic estimates of potential rock avalanche runout has been developed. To support this work, a regional dataset of 49 rock avalanches from the Canadian Cordillera was compiled through literature review and GIS-based mapping. Quantitative and qualitative descriptions of the events were made using attributes that are descriptive, yet simple enough to allow for larger grouping of events. Statistical analyses of the data indicated that treating volume and fall height as independent predictors of runout distance significantly improves the regression strength, relative to the more common method of using volume as a predictor of the angle of reach. The travel distance regression residuals show strong

stratification on the basis of path topography, and a weaker stratification on the basis of path substrate. A multiple linear regression accounting for whether or not there is lateral confinement along the runout path was generated. The mean path width of the deposit is proposed as a simple estimate of spreading, which can be estimated with good statistical strength using the event volume.

The regression analysis for runout distance predicted from fall height, event volume and confinement, and an independent analysis of the mean path width predicted from event volume were implemented into the PRE-RA screening-level predictive tool. The tool can be used to estimate the runout exceedance probability and the mean path width exceedance probability along a user-specified path or to estimate a volume that results in a specified runout exceedance probability at a specified point. The probabilistic output was developed with risk-based decision-making in mind and ease of use by practitioners involved in estimating landslide impact hazards. The screening-level information provided by the tool could be applied to provide preliminary estimates of spatial impact probability in a hazard or risk assessment and to determine if more detailed investigation and numerical modelling is warranted. If more detailed numerical modelling is pursued, this analysis could help constrain the volumes and model domains considered.

Further work is underway to develop a larger database of worldwide events described in a consistent manner. This would allow for more robust statistical analyses and could be used to re-examine some of the weaker effects found in this study, which could in turn help to better define the relative importance of the attributes on mobility. Finally, a consistent global database could be used to test if distinct regional trends can be observed.

## Acknowledgements

The authors would like to acknowledge the contributions of Nafis Jalal and Damian McClarty in compiling case studies and carrying out initial data analysis for preliminary stages of the work presented here. We would also like to thank Professor Brett Eaton for his assistance with the GIS and digitization tools in R used for the development of the predictive tool. Tom Millard with the BC Ministry of Forests, Land, Natural Resource Operations and Rural Development provided photos used for the May 13, 2019 Joffre Peak rock avalanche, and helicopter access to obtain photos after the May 16, 2019 Joffre Peak rock avalanche. Two anonymous reviewers provided helpful edits and suggestions that improved the final paper.

*Code and data availability* The PRE-RA code, raw data used to fit the regressions and a read-me file are available at: <https://github.com/admitchell/PRE-RA>. Shapefiles for the case histories are available through the DesignSafe-CI repository (Mitchell 2019).

## Funding information

We acknowledge the support of the Natural Sciences and Engineering Research Council of Canada (NSERC), funding reference number PGSD3 - 516701 - 2018.

## References

- Aaron JB, McDougall SD (2019) Rock avalanche mobility: the role of path material. *Eng Geol* 257: Article 105126.
- Blue Marble Geographics (2018) Global Mapper v19. Blue Marble Geographics, Hallowell

- Boulton N, Stead D, Schwab J, Geertsema M (2006) The Zymoetz River rock avalanche, June 2002, British Columbia, Canada. *Eng Geol* 83(1):76–93
- Christen M, Bühler Y, Bartelt P, Leine R, Glover J, Schweizer A, Graf C, McArdell BW, Gerber W, Deubelbeiss Y, Feistl T, Volkwein A (2012) Integral hazard management using a unified software environment: numerical simulation tool “RAMMS” for gravitational natural hazards. Dans: Koblotschnig, G.; Hübl, J.; Braun, J. (eds.) 12th Congress INTERPRAEVENT, Volume 1 pp. 77–86.
- Clague JJ (2000) Recognizing order in chaotic sequences of Quaternary sediments in the Canadian Cordillera. *Quat Int* 68-71:29–38
- Clague JJ (2017) Deglaciation of the Cordillera of Western Canada at the end of the Pleistocene. *Cuadernos de Investigacion Geografica* 43:449–466
- Corominas J (1996) The angle of reach as a mobility index for small and large landslides. *Can Geotech J* 33(2):260–271
- Cruden DM, Hungr O (1986) The debris of the Frank Slide and theories of rockslide – avalanche mobility. *Can J Earth Sci* 23:425–432
- Cruden DM, Krahn J (1973) A reexamination of the geology of the Frank Slide. *Can Geotech J* 10(4):581–591
- Friele P, Millard T, Mitchell A, Allstadt K, Menounos B, Geertsema M, Clague JJ (In Press) Initial observations of the May 2019 Joffre Peak rock avalanches, British Columbia. *Landslides*
- Griswold JP, Iverson RM (2008) Mobility statistics and automated hazard mapping for debris flows and rock avalanches. USGS Scientific Investigations Report 2007-5276
- Guthrie RH, Friele P, Allstadt K, Roberts N, Evans SG, Delaney KB, Roche D, Clague JJ, Jakob M (2012) The 6 August 2010 Mount Meager rock slide-debris flow, Coast Mountains, British Columbia: characteristics, dynamics, and implications for hazard and risk assessment. *Nat Hazards Earth Syst Sci* 12:1277–1294
- Heim A (1932) Landslides and human lives (Bergsturz und Menschenleben). Translated by N. Skermer, BiTech Publishers, Vancouver, BC, Canada
- Hermanns RL, Oppikofer T, Anda E, Blikra LH, Bohme M, Bunkholt H, Crosta GB, Dahle H, Devoli G, Fisher L, Jaboyedoff M, Loew S, Saetre S, Molina FY (2012) Recommended hazard and risk classification system for large unstable rock slopes in Norway. *Norges Geologiske Undersøkelse Report* 2012.029
- Horton P, Jaboyedoff M, Rudaz B, Zimmermann M (2013) Flow-R, a model for susceptibility mapping of debris flows and other gravitational hazards at a regional scale. *Nat Hazards Earth Syst Sci* 13:869–885
- Hsü KJ (1975) Catastrophic debris streams (sturzstroms) generated by rockfalls. *Geol Soc Am Bull* 86:129–140
- Hungr O, Evans S (1993) The failure behavior of large rockslides in mountainous regions. Geological Survey of Canada Open File Report 2598
- Hungr O, Evans S (2004) Entrainment of debris in rock avalanches: an analysis of a long run-out mechanism. *Geol Soc Am Bull* 116:1240–1252
- Hungr O, McDougall S (2009) Two numerical models for landslide dynamic analysis. *Comput Geosci* 35:978–992
- Hungr O, Leroueil S, Picarelli L (2014) The Varnes classification of landslide types, an update. *Landslides* 11(2):167–194
- Legros F (2002) The mobility of long-runout landslides. *Eng Geol* 63:301–331
- Li T (1983) A mathematical model for predicting the extent of a major rockfall. *Z Geomorphol* 24:473–482
- Matthews WH, McTaggart KC (1978) Hope Rockslides, British Columbia, Canada. In *Rockslides and Avalanches, 1: Natural Phenomena*, B Voight (ed). Elsevier
- McDougall S (2017) 2014 Canadian Geotechnical Colloquium: landslide runout analysis – current practice and challenges. *Can Geotech J* 54(5):605–620
- Mergili M, Krenn J, Chu H-J (2015) r.randomwalk v1, a multi-functional conceptual tool for mass movement routing. *Geosci Model Dev* 8:4027–4043
- Mergili M, Fischer J-T, Krenn J, Pudasaini SP (2017) r.avaflo w v1, an advanced open-source computational framework for the propagation and interaction of two-phase mass flows. *Geosci Model Dev* 10:553–569
- Mitchell A, McDougall S, Brideau M-A, Whittall J, McClarty D (2018) New empirical-statistical tools for the analysis of rock avalanche runout. 7th Canadian Geohazards Conference, Canmore, Canada. Paper 144
- Monger J, Price R (2002) The Canadian Cordillera: geology and tectonic evolution. *CSEG Recorder* 27(2):17–36
- Mitchell, A. Canadian Cordillera Rock Avalanche Case Histories. *DesignSafe-CI*, <https://doi.org/10.17603/ds2-vnk2-wz34> (2019).
- Nicoletti PG, Sorriso-Valvo M (1991) Geomorphic controls of the shape and mobility of rock avalanches. *Geol Soc Am Bull* 103:1365–1373
- Orwin JF, Clague JJ, Gerath RF (2004) The Cheam rock avalanche, Fraser Valley, British Columbia, Canada. *Landslides* 1:289–298
- Planet Team (2017) Planet application program interface: in space for life on earth. San Francisco, CA. <https://api.planet.com>
- R Core Team (2018) R: A language and environment for statistical computing. R Foundation for Statistical Computing, Vienna, Austria. <http://www.R-project.org/>
- Scheidegger AE (1973) On the prediction of the reach and velocity of catastrophic landslides. *Rock Mech* 5(4):231–236
- Simoni A, Mammoliti M, Berti M (2011) Uncertainty of debris flow mobility relationships and its influence on the prediction of inundated areas. *Geomorphology* 132:249–259
- Strom A, Li L, Lan H (2019) Rock avalanche mobility: optimal characterization and the effects of confinement. *Landslides* 16:1437–1452
- Wang SN, Xu WY, Shi C, Chen HJ (2017) Run-out prediction and failure mechanism analysis of the Zhenggang deposit in southwestern China. *Landslides* 14:719–726
- Whittall J, Eberhardt E, McDougall S (2017) Runout analysis and mobility observations for large open pit slope failures. *Can Geotech J* 54:373–391
- Xu X, Jin F, Sun Q, Soga K, Zhou GD (2019) Three-dimensional material point method modelling of the runout behaviour of the Hongshiyuan landslide. *Can Geotech J*. <https://doi.org/10.1139/cgj-2017-0638>
- Young DS (2017) *Handbook of Regression Methods*. CRC Press, Boca Raton
- Zhan W, Xuanmei F, Huang R, Pei X, Xu Q, Weile L (2017) Empirical prediction for travel distance of channelized rock avalanches in the Wenchuan earthquake area. *Nat Hazards Earth Syst Sci* 17:833–844

Electronic supplementary material The online version of this article (<https://doi.org/10.1007/s10346-019-01331-3>) contains supplementary material, which is available to authorized users.

**A. Mitchell** (✉) · **S. McDougall**

Department of Earth, Ocean and Atmospheric Sciences,  
University of British Columbia,  
2020 Earth Sciences Building, 2207 Main Mall, Vancouver, Canada  
Email: amitchell@eoas.ubc.ca

**N. Nolde**

Department of Statistics,  
University of British Columbia,  
3182 Earth Sciences Building, 2207 Main Mall, Vancouver, Canada

**M.-A. Brideau**

Institute of Geological and Nuclear Sciences Limited (GNS Science),  
1 Fairway Drive, Avalon, New Zealand

**J. Whittall**

BGC Engineering Inc.,  
Suite 500, 980 Howe Street, Vancouver, Canada

**J. B. Aaron**

ETH Zürich,  
Sonneggstrasse 5, 8092, Zürich, Switzerland